HHS Public Access

Author manuscript

J Long Term Eff Med Implants. Author manuscript; available in PMC 2019 September 04.

Published in final edited form as:

J Long Term Eff Med Implants. 2015 ; 25(1-2): 41–53.

On the Bending Properties of Porcine Mitral, Tricuspid, Aortic, and Pulmonary Valve Leaflets

Bryn Brazile[a], **Bo Wang**[a], **Guangjun Wang**[a], **Robbin Bertucci**[a], **Raj Prabhu**[a], **Sourav S. Patnaik**[a], **J. Ryan Butler**[b], **Andrew Claude**[b], **Erin Brinkman-Ferguson**[b], **Lakiesha N. Williams**[a], **Jun Liao**[a,*]

[a]Tissue Bioengineering Laboratory, Department of Biological Engineering, Mississippi State University, MS, 39762;

[b]Department of Clinical Sciences, College of Veterinary Medicine, Mississippi State University, MS, 39762

Abstract

The atrioventricular valve leaflets (mitral and tricuspid) are different from the semilunar valve leaflets (aortic and pulmonary) in layered structure, ultrastructural constitution and organization, and leaflet thickness. These differences warrant a comparative look at the bending properties of the four types of leaflets. We found that the moment–curvature relationships in atrioventricular valves were stiffer than in semilunar valves, and the moment–curvature relationships of the left-side valve leaflets were stiffer than their morphological analog of the right side. These trends were supported by the moment–curvature curves and the flexural rigidity analysis (*EI* value decreased from mitral, tricuspid, aortic, to pulmonary leaflets). However, after taking away the geometric effect (moment of inertia *I*), the instantaneous effective bending modulus *E* showed a reversed trend. The overall trend of flexural rigidity (*EI*: mitral > tricuspid > aortic > pulmonary) might be correlated with the thickness variations among the four types of leaflets (thickness: mitral > tricuspid > aortic > pulmonary). The overall trend of the instantaneous effective bending modulus (*E*: mitral < tricuspid < aortic < pulmonary) might be correlated to the layered fibrous ultrastructures of the four types of leaflets, of which the fibers in mitral and tricuspid leaflets were less aligned, and the fibers in aortic and pulmonary leaflets were highly aligned. We also found that, for all types of leaflets, moment–curvature relationships are stiffer in against-curvature (AC) bending than in with-curvature bending (WC), which implies that leaflets tend to flex toward their natural curvature and comply with blood flow. Lastly, we observed that the leaflets were stiffer in circumferential bending compared with radial bending, likely reflecting the physiological motion of the leaflets, i.e., more bending moment and movement were experienced in radial direction than circumferential direction.

Keywords

mitral valve leaflets; tricuspid valve leaflets; aortic valve leaflets; pulmonary valve leaflets; bending properties; moment–curvature relationships; heart valve biomechanics

[*]Address all correspondence to: Jun Liao, PhD, Tissue Bioengineering Laboratory, Department of Biological Engineering, Mississippi State University, Mississippi State, MS 39762; Tel: 662-325-5987, Fax: 662-325-3853, jliao@abe.msstate.edu.

I. INTRODUCTION

The heart is responsible for pumping more than 7,000 liters of blood through the body daily. This causes the heart valves, i.e., two atrioventricular valves (mitral valve and tricuspid valve) and two semilunar valves (aortic valve and pulmonary valve), to open and close more than 3×10^9 times during a typical lifetime. All four valves open and close in a highly coordinated way by responding to blood pressure changes in both upstream and downstream locations, and hence they maintain unidirectional blood flow of cardiac circulation.

The mechanical loading that the heart valves experience is complicated and nonstop. During the opening and closing cycle, the leaflets of the four types of valves all experience dynamic and complex mechanical stresses and corresponding large deformations.[1,2] The leaflets must contend with bending when the valves open and close, with shear stress due to blood flow that occurs while the valves are open, and with tension that occurs when the valves are closed under backward pressure gradients. The complicated deformation/motion pattern and boundary condition require valvular tissues with optimal structure design that are able to smoothly handle large deformations as bending, stretch, and shear, without incurring internal structural damage. Fortunately, the natural design of the heart valves allows the valvular tissues to be durable over the lifetime and manage the mechanical challenges well; however, due to many other factors, heart valve diseases still have a relatively high prevalence and afflict functionality of the heart.[1–3]

According to the American Heart Association, 22,144 people died from valvular heart disease in 2009.[4] It is estimated that valvular heart disease affects 2.5% of the US population, and the prevalence of valvular diseases increases as a person ages.[5] Valvular heart disease can occur in any single valve or a combination of the four valves. The most common valvular diseases are aortic valve stenosis, aortic valve regurgitation, mitral valve stenosis, and mitral valve regurgitation. Other valvular diseases are pulmonary valve stenosis, pulmonary valve regurgitation, tricuspid valve stenosis, and tricuspid valve regurgitation.[4,6–9]

As we mentioned above, the delicately designed valvular leaflets experience shear, tension, and flexure every time the valve opens and closes.[10–12] To better understand the physiological and patho-physiological behavior of heart valves, mechanical properties of valvular tissues in both normal and diseased conditions must be quantified and analyzed thoroughly.[1,13–16] Biaxial mechanical tests have been applied to reveal valvular tissue behavior under physiologically relevant loading conditions.[10–12,17–21] Uniaxial mechanical tests also provide important information about failure strain and strength of valvular tissues. Talman *et al.* also developed a shear testing device to characterize the shear properties in aortic valve leaflets.[22–24] To investigate valve flexural behavior, Sacks *et al.* studied the bending properties of aortic valve leaflets and pulmonary valve leaflets using custom made simple bending and three-point bending setups. They found that valvular flexural properties were very sensitive to chemical treatment, cellular contraction, collagen fiber architecture, and other factors.[2,10,11,21,25–28] To date, no study has been done to investigate the flexural

properties of mitral valve leaflets and tricuspid valve leaflets, of which bending is the essential part of valvular deformation during the cycle of opening and closing.[29–33]

Another interesting observation is that the layered structure of mitral valve leaflets and tricuspid valve leaflets are very different from aortic and pulmonary valve leaflets. Both aortic valves and pulmonary valves have three semilunar leaflets, with the pulmonary valve leaflet being the thinnest leaflet and the aortic valve the second thinnest of the four types of heart valves. The layered structure of the aortic valve leaflet and pulmonary leaflet is the same, i.e., (1) a fibrosa layer, mainly composed of circumferentially oriented type I collagen fibers, faces upward toward the aorta or pulmonary artery; (2) a spongiosa layer largely composed of proteoglycans (PGs)/glycosaminoglycans (GAGs) as the middle cushion layer; and (3) a ventricularis layer, mainly composed of radially oriented elastin fibers, faces downward toward the left or right ventricle.[12,34,35]

Different from the aortic valve and the pulmonary valve, the mitral valve consists of two leaflets, i.e., a large scallop-shaped anterior leaflet and a smaller posterior leaflet, and the tricuspid valve consists of three leaflets, i.e., a large anterior leaflet, a middle-sized medial leaflet, and a small posterior leaflet. The mitral valve leaflet is the thickest, and the tricuspid valve leaflet is the second thickest of the four types of heart valves. Mitral and tricuspid valve leaflets have a similar layered structure. Facing the left atrium or right atrium is the thin atrialis layer, which mainly consists of elastin fibers; in the middle, is the spongiosa layer composed of mainly PGs/GAGs; facing the left or right ventricle is a thick fibrosa layer predominantly made of a dense collagen fiber network.[30,26–40]

The differences of the valve leaflets in layered structure, ultrastructural constitution and organization, and leaflet thickness warrants a comparative look at bending properties of the four types of valves at once. Moreover, flexural properties and parameters can be an important input for computational modeling and simulations that aim to capture in vivo valvular tissue behavior with a high accuracy. In this study, we measured and compared the bending properties of the four types of valve leaflets in a thorough manner. This study has provided insight into various flexural behaviors of the four types of valve leaflets as well as a complete dataset in valvular flexure. These results can be applied to future studies in the field of heart valve biomechanics and computational simulation.

II. MATERIALS AND METHODS

A. Tissue Preparation

Porcine hearts from healthy pigs (~6 months) were obtained from a local abattoir. The specimens were stored in phosphate-buffered saline solution (PBS) at 4°C soon after extraction and were transported to the laboratory. For this study, the aortic valve leaflets and pulmonary leaflets were harvested for bending testing; for mitral valve and tricuspid valve, only anterior leaflets were harvested and used for bending testing. Tissue strips were dissected out of the aortic and pulmonary leaflets either along the circumferential direction or the radial direction with a dimension of 8 mm in length and 4 mm in width. Due to the relatively large size of the anterior leaflets of mitral valve and tricuspid valve, the tissue strips were harvested from the central belly region with similar 8 mm length × 4 mm width,

either along the circumferential direction or radial direction. The dimensions of the leaflet strips, i.e., length, width, and thickness were measured using a digital calipers. For strip thickness, three thickness measurements were taken evenly along the length to estimate the average thickness.

B. Bending Mechanical Testing

A simple bending system was custom built for this study. The overall experimental setup followed the design scheme published by Sacks *et al.*[2] Briefly, the ends of the leaflet strip were glued to two small, hollow tubes (4 mm length). For aortic valve and pulmonary leaflets, the tissue strip was then mounted with the ventricularis side upward and the fibrosa side downward; for mitral valve and tricuspid valve leaflets, the tissue strip was mounted with the atrialis side upward and the fibrosa side downward. Via one hollow tube, one end of the tissue strip was mounted onto a stainless steel wire post that was fixed on one side wall of the bath chamber, whereas another end of the tissue strip was mounted to an L-shaped bending bar by sliding the hollow tube onto the short horizontal tip of the bending bar. The bath chamber was set on a linear positioner controlled by a Velmex stepper motor (Velmex, Inc., Bloomfield, NY). Hence, by moving the bath chamber we were able to bend the leaflet strip, and the calibrated bending bar was also deflected and could be tracked for force measurement. The bending bar was made of titanium wire (grade 23, Small Parts, Inc.), with a length of 14 cm (5.5 inches), and a diameter of 0.38 mm (0.015 inches). Five dark contrast markers were used for track ing the leaflet strip curvature. Marker 1 was pasted on the fixed post, markers 2 to 4 were pasted along the edge of the tissue strip, and marker 5 was pasted on the end of the bending bar. The five markers were distributed in even intervals along the strip length. A fithe le camera (DMK21AF04 model, The Imaging Source) was used to capture the movement of the markers during the bending procedure.

A LabView program (version 2000, National Instrument) was custom written to operate the Velmex stepper motor, the firewire camera image capturing, image thresholding, marker tracking, and output of the marker coordinates dataset. The output dataset had the information of marker positions of each image frame during the bending procedure. A MathCAD program was written to further process the output dataset by calculating the force recorded by the bending bar and hence the bending moment (M), and the resulted change in leaflet strip curvature ($\Delta\kappa$).

As previously reported by Sacks *et al.*,[2,21,25–28] the Euler-Bernoulli equation can be used for the moment–curvature relationship,

$$M = EI\,\Delta\kappa, \quad (1)$$

where M is the bending movement, $\Delta\kappa$ is the resulted change in curvature, E is the instantaneous effective bending modulus, I is moment of inertia calculated as follows:

$$I = \frac{1}{12} wt^3, \quad (2)$$

where w is the width and t is the thickness of the tissue strip, respectively. The EI gives an estimation of flexural rigidity.

C. Bending Testing Protocols

The bending tests of the four types of valve leaflets are summarized as follows. For each type of valve, the leaflet strips along both the circumferential and radial direction were measured. Notably, the aortic valve leaflet and pulmonary valve leaflet has a natural curvature that points from ventricularis layer to fibrosa layer (follow the blood flow direction). For mitral valve leaflet and tricuspid valve leaflet, the natural curvature is not as obvious as the aortic and pulmonary valve leaflets, but the flexural direction has a similar pattern that points from the atrialis layer to fibrosa layer (follow the blood flow direction). For aortic and pulmonary valve leaflets, we followed the routine set by Sacks *et al.* to flex each leaflet strip in two directions, i.e., "with curvature (WC)," which subjected the ventricularis to tension, and "against curvature (AC)," which subjected the fibrosa to tension. For mitral and tricuspid valve leaflets, we flexed each leaflet strip using a similar way, i.e., we defined a "with curvature (WC)" direction, which subjected the atrialis layer to tension, and an "against curvature (AC)" direction, which subjected the fibrosa layer to tension.

D. Histology and Scanning Electron Microscopy

To reveal the layered structure, the four types of leaflets were submerged in 10% neutral buffered formalin for fixation. Samples were kept submerged for 3 hours and then placed in fresh formalin in a 4° C refrigerator for at least 72 hours before histological sample preparation. Histological slides were stained with Movat's pentachrome, of which collagen was stained as a yellow color, GAGs stained as a blue color, and elastin stained as a black color.

Scanning electron microscopy (SEM) was performed to further reveal the ultrastructure of the four types of leaflets. Our goal was to examine the fiber orientation and alignment of the fibrosa and ventricularis/atrialis layers of each of the four types of valve leaflets. Leaflet samples were carefully cut into a rectangular shape with one edge aligned along circumferential direction and the other edge along radial direction. The endothelial cells on the leaflet surface were carefully removed by scalpel blade scrapping. The leaflet samples were then submersed in 2.5% formalin for more than 72 hours for fixation. The leaflet samples were dehydrated in a graded ethanol series, followed by critical point drying (Polaron E 3000 CPD) and sputter coated with gold–palladium. For each type of leaflet, both the fiallad and ventricularis/atrialis surface were observed and imaged with SEM (JEOL JSM-6500 FE-SEM).

E. Statistical Analysis

Statistical analysis was performed using SigmaPlot version 12 (Systat Software, Inc., San Jose, CA). For each examined curvature value (0.025 mm^{-1}, 0.05 mm^{-1} and 0.075 mm^{-1}), the corresponding EI and E values for each strip orientation (circumferential and radial) and bending direction (WC and AC) were compared among the four types of leaflets. Kruskal-Wallis non-parametric test was performed to determine significant differences among the four types of leaflets. Data was considered statistically significant when $p < 0.05$.

III. RESULTS

When the leaflet strips were examined along the circumferential direction, we found that all four types of valves showed a nonlinear momentum–curvature relationship when bent with the natural curvature (WC); however, when bent against curvature (AC) the four types of valves showed less nonlinearity, especially the aortic valve leaflet which appeared almost as a linear relationship (Fig. 1). The linearity relationship of aortic valve in AC bending was consistent with the previous report by Mirnajafi and Sacks *et al.*[27,41] Note that the observed moment-curvature values of the aortic and pulmonary leaflets fell into the similar range of that reported in the literature.[2,21]

For all four types of valve leaflets, the AC moment–curvature relationship appeared stiffer than the WC moment–curvature relationship when tested in the circumferential direction. When each of the valve leaflets was compared to one another in terms of moment-curvature relationship, the mitral valve leaflet was the stiffest, next the tricuspid valve leaflet, then the aortic valve leaflet, and finally the pulmonary valve leaflet (Fig. 1).

For the leaflet strips cut along the radial direction, we found that all four types of valves showed a nonlinear momentum–curvature relationship when bent along WC and AC. For the overall moment–curvature relationship, we still observed a decrease trend from mitral valve leaflet to tricuspid valve leaflet to aortic valve leaflet to finally the pulmonary valve leaflet. When comparing WC with AC bending of radial direction for each type of valve leaflets, we found that for the four types of valve leaflets the AC bending was still stiffer than the WC bending. We also noticed that, for aortic valve and pulmonary valve leaflet AC bending, the increasing trend of the moment–curvature curve obviously slowed down after the curvature value went past ~0.1 mm^{-1}. This phenomenon was not seen in WC bending of the aortic and pulmonary valve leaflets (Fig. 2).

Our results were reorganized in Fig. 3 to specifically compare the moment–curvature relationships of the circumferential and radial directions in each type of valve leaflet. Overall, for all four types of leaflets circumferential direction moment–curvature curves were stiffer than the radial direction moment–curvature for both WC bending and AC bending (Fig. 3). We also noted that, for the pulmonary valve leaflets, the circumferential and radial moment–curvature curves largely overlapped in AC bending (Fig. 3d).

We further analyzed the flexural rigidity (EI) and the instantaneous effective bending modu lus (E) of the four types of valve leaflets. To show the trend at a quantitative way, EI and E were calculated at $\Delta\kappa = 0.025\ mm^{-1}$, $\Delta\kappa = 0.05\ mm^{-1}$, and $\Delta\kappa = 0.075\ mm^{-1}$ and listed in Table 1 and Table 2, respectively. Reflecting the observation on the moment–curvature relationship, the flexural rigidity, EI, showed a decreasing trend from the mitral valve, tricuspid valve, aortic valve, to pulmonary valve leaflets (Table 1). Interestingly, after taking away the geometric effect (moment of inertia $I = \frac{1}{12}wt^3$), the instantaneous effective bending modulus E showed an opposite trend, in which the pulmonary valve leaflet showed the highest E, the aortic valve leaflet as the second highest, followed by the tricuspid valve leaflet, and finally the mitral valve leaflet with lowest E (Table 2).

For each examined curvature (0.025 mm^{-1}, 0.05 mm^{-1}, and 0.075 mm^{-1}), *EI* and *E* values obtained against curvature (AC) in either circumferential or radial directions were found to be signifi cantly different ($p < 0.05$) among the four types of valve leaflets. Similarly, for WC bending in either circumferential or radial direction, *EI* and *E* values were found to be significantly different ($p < 0.05$) among the four types of valve leaflets, except *EI* of circumferential WC bending.

The layered structure of the four types of heart valve leaflets was shown in Fig. 4. The atrialis, spongiosa, and fibrosa layers were observed in the mitral valve and tricuspid valve leaflets (Fig. 4a,b), in which the major black stains for elastin fibers were abundant in the atrialis layer, the blue stains were abundant for GAG content in the spongiosa layer, and the yellow stains were abundant for the dominate collagen composition in the fibrosa layer. The fibrosa, spongiosa, and ventricularis layers were also observed in the aortic and pulmonary leaflets (Fig. 4-c,d), in which the yellow stains for the dense collagen network in the fiere a layer, the blue color stains for the GAG content in the spongiosa layer, and the black stains for the elastin fibers in the ventricularis layer.

Fiber orientation and alignment were examined using SEM images taken on the fibrosa layer and ventricularis/atrialis layers. We showed that, for mitral and tricuspid valve leaflets, the fiber orientation was more random and fiber alignment was more spread out (Fig. 5a,b,e,f) than those of the aortic and pulmonary valve leaflets. For aortic and pulmonary valve leaflets, similar to findings reported in previous studies,[21,35] we found that the fibers in the fibrosa surface (mostly collagen) were dominantly running along the circumferential direction with a high degree of alignment (Fig. 5c,d), and the fibers in the ventricularis surface (mostly elastin) were found mostly running along the radial direction (Fig. 5g,h). Notably, SEM cannot distinguish the difference between collagen and elastin fibers; moreover, Fig. 5 shows only fibers on the surface layer. But the trends of fiber orientation and alignment shown in Fig. 5 reflect the overall characteristics of the fibers spatial distributions across the layer thickness and are supported by other reports in the literature.[21,35]

IV. DISCUSSION

A. Moment–Curvature Comparison among Valve Types

We found that the moment–curvature relationships in atrioventricular (mitral and tricuspid) valves were stiffer than semilunar (aortic and pulmonary) valves. This phenomenon likely reflects the underlying structural difference considering the increased thickness of the atrioventricular valves compared with semilunar valves. Moreover, we found that left-side heart valves were stiffer than their morphological analog in the right side of the heart (i.e., the mitral is stiffer than tricuspid and the aortic is stiffer than the pulmonary). This finding correlates well with our existing understanding of the mechanical environment of the heart, i.e., the pressures and mechanical loads in the left side of the heart are much greater than those in the right side of the heart.[8,16] Our observation of overall trend of moment–curvature relationships in the four types of valve leaflets is reinforced by the thickness differences among the four types of valves; the mitral valve anterior leaflet is thicker than the tricuspid

valve anterior leaflet, and the aortic valve leaflet is thicker than the pulmonary valve leaflet.[21,27,29,30,33,35,38,42]

B. Moment–Curvature Comparison between WC and AC Bending

We noticed that, overall, heart valves are stiffer in bending against their natural curvature (AC bend ing) than with their natural curvature (WC bending) (Fig. 6). This relationship holds true for all four types of valves, in both radial and circumferential directions. This finding is important and interesting when closely examining the bending behavior of heart valve leaflets. To wit, heart valves are able to bend toward their natural curvature and comply with blood flow but resist bending against their natural curvature, likely to prevent prolapse and backflow.

For WC bending, the fibrosa layer (mainly collagen fibers) of the four types of leaflet was subjected to compression; whereas the atrialis layer (mainly elastin fibers) in mitral and tricuspid valve and ventricularis layer (mainly elastin fibers) in aortic and pulmonary valve was subjected to tension. For AC bending, the layered behavior was totally inversed, of which the filayer layer of the four types of leaflets was subjected to tension, and the atrialis in mitral and tricuspid valves and ventricularis in aortic and pulmonary valves were subjected to compression. From a material point of view, dominant elastin fibers were subjected to tension in WC bending; in AC bending, dominant collagen fibers were subjected to tension. Therefore, considering the fact that in general elastin fibers were less stiff and largely more extensible than collagen fibers, it is reasonable to conclude that WC bending is less stiff than AC bending. However, for the detailed mechanistic analysis of this phenomenon, we considered the layered structure, as well as the thickness, composition, and fiber orientations and alignment of each layer in the four types of valve leaflets (Figs. 4 and 5).

C. Moment-Curvature Comparison between Circumferential Bending and Radial Bending

Figure 6 showed that, for all four types of valve leaflets, leaflet strips were stiffer in circumferential bending than radial bending. This trend might be related to the physiological motion of the valve leaflets, in which the radial direction seemly experiences more bending moment as well as bending movement than the circumferential direction. Another important difference between leaflet strips cut in the circumferential direction and cut in the radial direction was that the circumferential strip had a more uniform thickness along the strip length, whereas the radial strip had a relatively tapered thickness along the strip length. The degree of tapering was slightly obvious in aortic and pulmonary leaflets since the strips ran across most of the radial dimension. However, the tapering was barely noticeable in mitral and tricus pid leaflets because the strips were dissected from the central belly region. For radial bending of aortic and pulmonary leaflets, the tapering dimension, as well as the uneven surface in fibrosa layer, might also be factors contributing to the observed moment–curvature variation when comparing radial and circumferential direction bending.

The tapering in radially cut aortic and pulmonary leaflets seems to be a reason that only circumferential direction bending has been investigated up to now. Nevertheless, from a biomechanical perspective, the quantification of bending behavior in the radial direction is

still worthy of effort. Note that, for estimating the instantaneous effective bending modulus along the radial direction, average thickness of the leaflet strip was used for computation, and the resulted E value represents an overall estimation.

V. CONCLUSIONS

Our major observations are summarized as follows:

1. The moment–curvature relationships in atrioventricular valves were stiffer than semilunar valves, and the left-side heart valves were stiffer than their morphological analog in the right side of the heart. The difference in overall flexural rigidity (*EI*: mitral leaflet > tricuspid leaflet > aortic leaflet > pulmonary leaflet) might be related to the thickness variations among the four types of leaflets.
2. The instantaneous effective bending modulus, *E*, showed a reversed trend, of which *E* value took an increase order (*E*: mitral leaflet < tricuspid leaflet < aortic leaflet < pulmonary leaflet). The difference in *E* might be related to the layered fibrous ultrastructures of the four types of valve leaflets, of which the fibers in mitral and tricuspid leaflets were less aligned, and the fibers in aortic and pulmonary leaflets were highly aligned.
3. All types of leaflet moment–curvature relationships are stiffer in against-curvature (AC) bending than in with-curvature bending (WC), which implies that leaflets tend to flex toward their natural curvature and comply with blood flow, while they have a tendency to resist bending against their natural curvature.
4. The leaflets were stiffer in circumferential bending compared with radial bending; this finding likely reflects the physiological motion of the leaflets, of which more bending moment and movement were experienced in a radial direction than in a circumferential direction.

The complexity of the bending behavior of the four types of valve leaflets and the intriguing layered ultrastructures of various leaflets warrant future studies that aim to reveal the underlying mechanisms that cause the observed differences. Our hope is that the reported data can be helpful in better defining the physiological behavior and the long-term durability of heart valve leaflets, assisting more accurate computational modeling and simulation, as well as being incorporated into the development of heart valve replacements with a prolonged lifespan.

ACKNOWLEDGMENTS

This study was supported in part by American Heart Association (grant no. 13GRNT17150041), NIH National Heart, Lung, and Blood Institute (grant nos. HL097321, and NSF EPS-0903787). The authors thank Dr. Benjamin Weed for his invaluable discussion and Ms. Amanda Lawrence (I2AT) for her help with SEM imaging. Support from Sansing Meat Service (Maben, MS) is also greatly appreciated.

REEERENCES

1. Mendelson K, Schoen FJ. Heart valve tissue engineering: concepts, approaches, progress, and challenges. Ann Biomed Engineer. 2006;34(12):1799–819.

2. Merryman WD, Engelmayr GC Jr, Liao J, Sacks MS. Defining biomechanical endpoints for tissue engineered heart valve leaflets from native leaflet properties. Prog Pediatr Cardiol. 2006;21(2):153–60.

3. Schoen F, Edwards W. Valvular heart disease: general principles and stenosis. Cardiovasc Pathol. 2001;3:403–42.

4. Go AS, Mozaffarian D, Roger VL, Benjamin EJ, Berry JD, Borden WB, et al. Heart disease and stroke statistics—2013 update a report from the American Heart Association. Circulation. 2013;127(1):e6–e245. [PubMed: 23239837]

5. Nkomo VT, Gardin JM, Skelton TN, Gottdiener JS, Scott CG, Enriquez-Sarano M. Burden of valvular heart diseases: a population-based study. Lancet. 2006;368(9540):1005–11. [PubMed: 16980116]

6. Roger VL, Go AS, Lloyd-Jones DM, Benjamin EJ, Berry JD, Borden WB, et al. Heart disease and stroke statistics—2012 update a report from the American Heart Association. Circulation. 2012;125(1):e2–e220. [PubMed: 22179539]

7. Nishimura RA. Aortic valve disease. Circulation. 2002;106(7):770–2. [PubMed: 12176943]

8. Lilly LS. Pathophysiology of heart disease: a collaborative project of medical students and faculty. Wolters Kluwer Health; 2012.

9. Takkenberg JJ, Rajamannan NM, Rosenhek R, Kumar AS, Carapetis JR, Yacoub MH. The need for a global perspective on heart valve disease epidemiology the shvd working group on epidemiology of heart valve disease founding statement. J Heart Valve Dis. 2008;17(1):135. [PubMed: 18365583]

10. Sacks MS, David Merryman W, Schmidt DE. On the biomechanics of heart valve function. J Biomechan. 2009;42(12):1804–24.

11. Sacks MS, Yoganathan AP. Heart valve function: a bio-mechanical perspective. Philos Trans Roy Soc Biol. 2007;362(1484):1369–91.

12. Christie GW, Barratt-Boyes BG. Mechanical properties of porcine pulmonary valve leaflets: How do they differ from aortic leaflets? Ann Thoracic Surg. 1995;60:S195–S9.

13. Breuer CK, Mettler BA, Anthony T, Sales VL, Schoen FJ, Mayer JE. Application of tissue-engineering principles toward the development of a semilunar heart valve substitute. Tissue Engineer. 2004;10(11–12):1725–36.

14. Schoen FJ. Evolving concepts of cardiac valve dynamics the continuum of development, functional structure, pathobiology, and tissue engineering. Circulation. 2008;118(18):1864–80. [PubMed: 18955677]

15. Rabkin-Aikawa E, Mayer JE Jr, Schoen FJ. Heart Valve Regeneration Regenerative Medicine II. Editor Yannas I, Heidelberg: Springer-Berlin 2005 94: 141–79

16. Katz A. Physiology of the heart. Philadelphia: Wolters Kluwer Health; 2011.

17. Billiar K, Sacks M. Biaxial mechanical properties of the natural and glutaraldehyde treated aortic valve cusp—part I: experimental results. Trans Am Soc Mechan Engineers J Biomech Engineer" to "Journal of Biomechanical Engineering. 2000;122(1):23–30.

18. Stella JA, Liao J, Sacks MS. Time-dependent biaxial mechanical behavior of the aortic heart valve leaflet. J Biomech. 2007;40(14):3169–77. [PubMed: 17570376]

19. Stella JA, Sacks MS. On the biaxial mechanical properties of the layers of the aortic valve leaflet. J Biomech Engineer. 2007;129(5):757.

20. May-Newman K, Yin F. Biaxial mechanical behavior of excised porcine mitral valve leaflets. Am J Physiol Heart. 1995;269(4):H1319–H27.

21. Liao J, Joyce EM, Sacks MS. Effects of decellularization on the mechanical and structural properties of the porcine aortic valve leaflet. Biomaterials. 2008;29(8):1065–74. [PubMed: 18096223]

22. Talman E, Boughner D. Internal shear properties of fresh aortic valve cusps: implications for normal valve function. J Heart Valve Dis. 1996;5:152–9. [PubMed: 8665007]

23. Talman EA, Boughner DR. Glutaraldehyde fixation alters the internal shear properties of porcine aortic heart valve tissue. Ann Thoracic Surg. 1995;60:S369–S73.

24. Vesely I, Boughner D. Analysis of the bending behaviour of porcine xenograft leaflets and of natural aortic valve material: bending stiffness, neutral axis and shear measurements. J Biomech. 1989;22(6/7):655–71. [PubMed: 2509479]
25. Nicosia MA. A theoretical framework to analyze bend testing of soft tissue. J Biomech Engineer. 2007;129:117.
26. Mirnajafi A, Raymer JM, McClure LR, Sacks MS. The flexural rigidity of the aortic valve leaflet in the commissural region. J Biomech.. 2006;39(16):2966–73. [PubMed: 16360160]
27. Mirnajafi A, Raymer J, Scott MJ, Sacks MS. The effects of collagen fiber orientation on the flexural properties of pericardial heterograft biomaterials. Biomaterials. 2005;26(7):795–804. [PubMed: 15350785]
28. Merryman DW, Shadow Huang HY, Schoen FJ, Sacks MS. The effects of cellular contraction on aortic valve leaflet flexural stiffness. J Biomech. 2006;39(1):88–96. [PubMed: 16271591]
29. Du Plessis LA, Marchand P. The anatomy of the mitral valve and its associated structures. Thorax. 1964;19(3):221–7. [PubMed: 14143500]
30. Ho S. Anatomy of the mitral valve. Heart. 2002;88(suppl 4):iv5–iv10. [PubMed: 12369589]
31. Eckert CE, Zubiate B, Vergnat M, Gorman JH III, Gorman RC, Sacks MS. In vivo dynamic deformation of the mitral valve annulus. Ann Biomed Engineer. 2009;37(9):1757–71.
32. Sacks MS, Enomoto Y, Graybill JR, Merryman WD, Zeeshan A, Yoganathan AP, et al. In-vivo dynamic deformation of the mitral valve anterior leaflet. Ann Thoracic Surg. 2006;82(4):1369–77.
33. Nii M, Roman KS, Macgowan CK, Smallhorn JF. Insight into normal mitral and tricuspid annular dynamics in pediatrics: a real–time three-dimensional echocardiographic study. J Am Soc Echocardiogr. 2005;18(8):805–14. [PubMed: 16084332]
34. Thubrikar M, Klemchuk PP. The aortic valve. Boca Raton, FL: CRC Press; 1990.
35. Joyce EM, Liao J, Schoen FJ, Mayer JE Jr, Sacks MS. Functional collagen fiber architecture of the pulmonary heart valve cusp. Ann Thoracic Surg. 2009;87(4):1240–9.
36. Gross L, Kugel M. Topographic anatomy and histology of the valves in the human heart. Am J Pathol. 1931;7(5):445. [PubMed: 19969978]
37. Bezerra A, DiDio L, Prates J. Dimensions of the left atrioventricular valve and its components in normal human hearts. Cardioscience. 1992;3(4):241–4. [PubMed: 1477291]
38. Anderson R, Becker A. Anatomy of the heart. Stuttgart, NY: Thieme 1982.
39. Misfeld M, Sievers H-H. Heart valve macro-and microstructure. Philos Trans Roy Soc Biol. 2007;362(1484):1421–36.
40. Grande-Allen KJ, Liao J. The heterogeneous biomechanics and mechanobiology of the mitral valve: implications for tissue engineering. Curr Cardiol Rept. 2011;13(2):113–20.
41. Sacks M, Gloeckner D, Vyavahare N, Levy R. Loss of flexural rigidity in bioprosthetic heart valves with fatigue: new findings and the relation to collagen damage. J Heart Valve Dis. 2001.
42. Tei C, Pilgrim J, Shah P, Ormiston J, Wong M. The tricuspid valve annulus: study of size and motion in normal subjects and in patients with tricuspid regurgitation. Circulation. 1982;66(3): 665–71. [PubMed: 7094278]

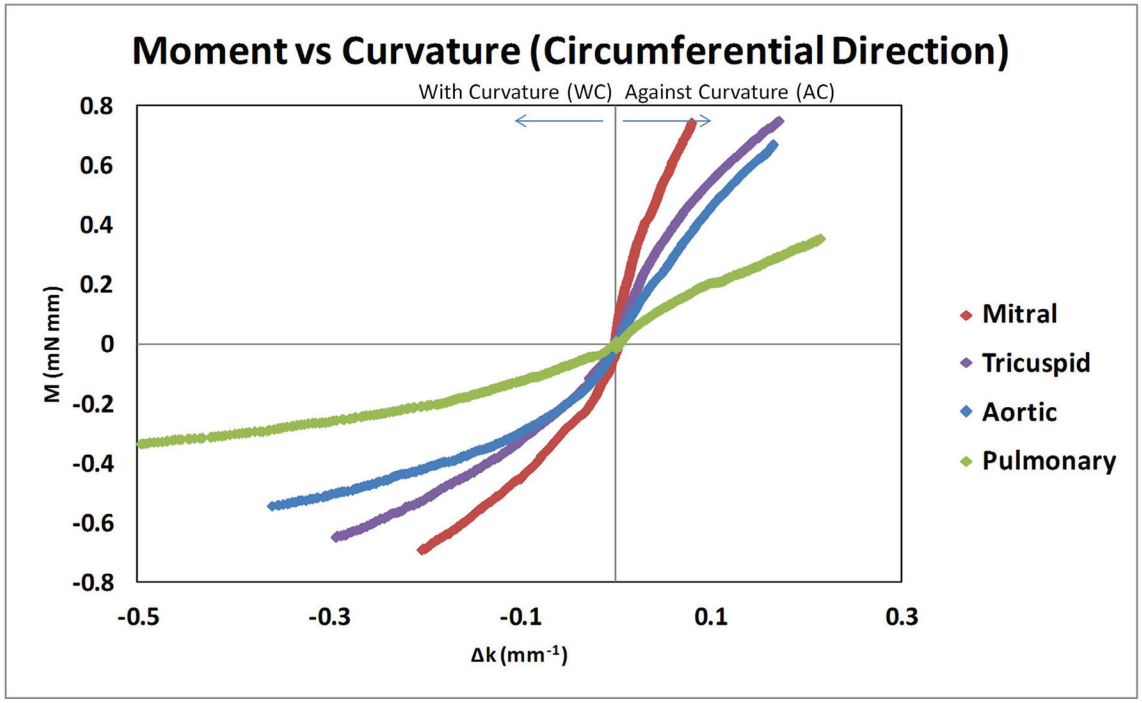

FIG. 1:

Circumferential direction moment–curvature relationships for mitral, tricuspid, aortic, and pulmonary valve leaflets. Both against curvature (AC) bending and with curvature (WC) bending were shown.

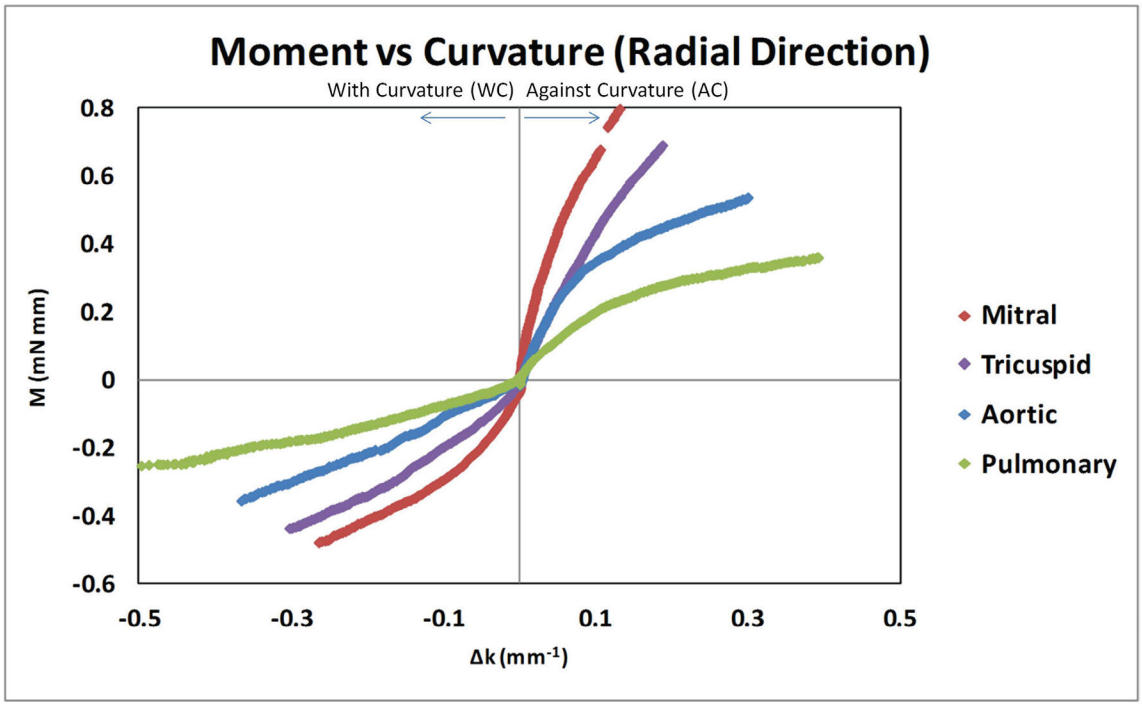

FIG. 2:

Radial direction moment–curvature relationships for mitral, tricuspid, aortic, and pulmonary valve leaflets. Both against curvature (AC) bending and with curvature (WC) bending were shown.

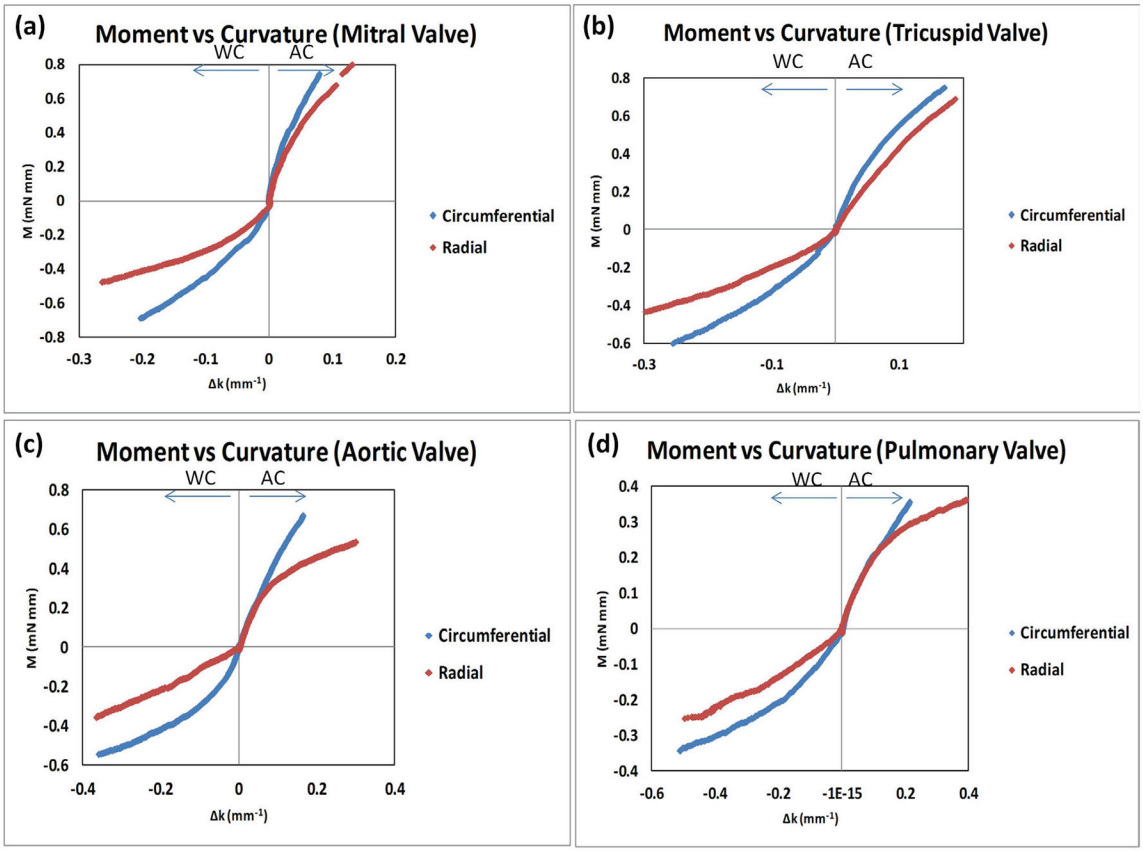

FIG. 3:

Data in Figure 1 and 2 were reorganized to specifically compare the moment–curvature relationships of the circumferential and radial directions: **(a)** mitral valve leaflets, **(b)** tricuspid valve leaflets, **(c)** aortic valve leaflets, and **(d)** pulmonary valve leaflets.

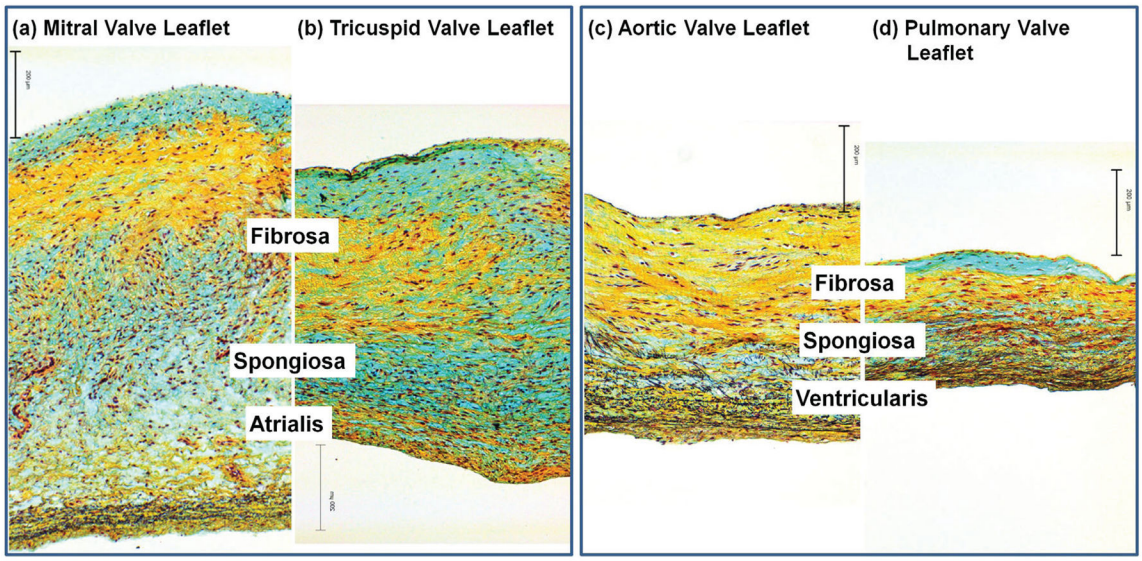

FIG. 4:

Histological comparison of **(a)** mitral valve leaflet, **(b)** tricuspid valve leaflet, **(c)** aortic valve leaflet, and **(d)** pulmonary valve leaflet. Note that, for mitral and tricuspid valve leaflets, the layered structure is fibrosa (facing ventricle), spongiosa, and atrialis (facing atrium); for aortic and pulmonary valve leaflets, the layered structure is fibrosa (facing aorta/pulmonary artery), spongiosa, and ventricularis (facing ventricle). Scale bar = 200 μm.

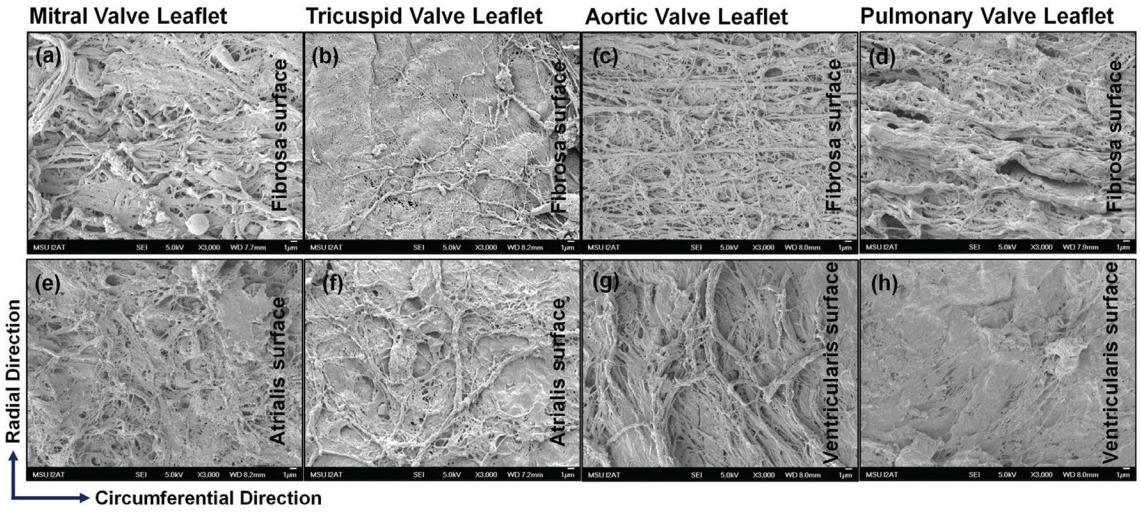

FIG. 5:

Ultrastructural comparison revealed by SEM: **(a)** fibrosa surface and **(e)** atrialis surface of mitral valve leaflet; **(b)** fibrosa surface and **(f)** atrialis surface of tricuspid valve leaflet; **(c)** fibrosa surface and **(g)** ventricularis surface of aortic valve leaflet; **(d)** fibrosa surface and **(h)** ventricularis surface of pulmonary valve leaflet. Scale bar = 1 μm.

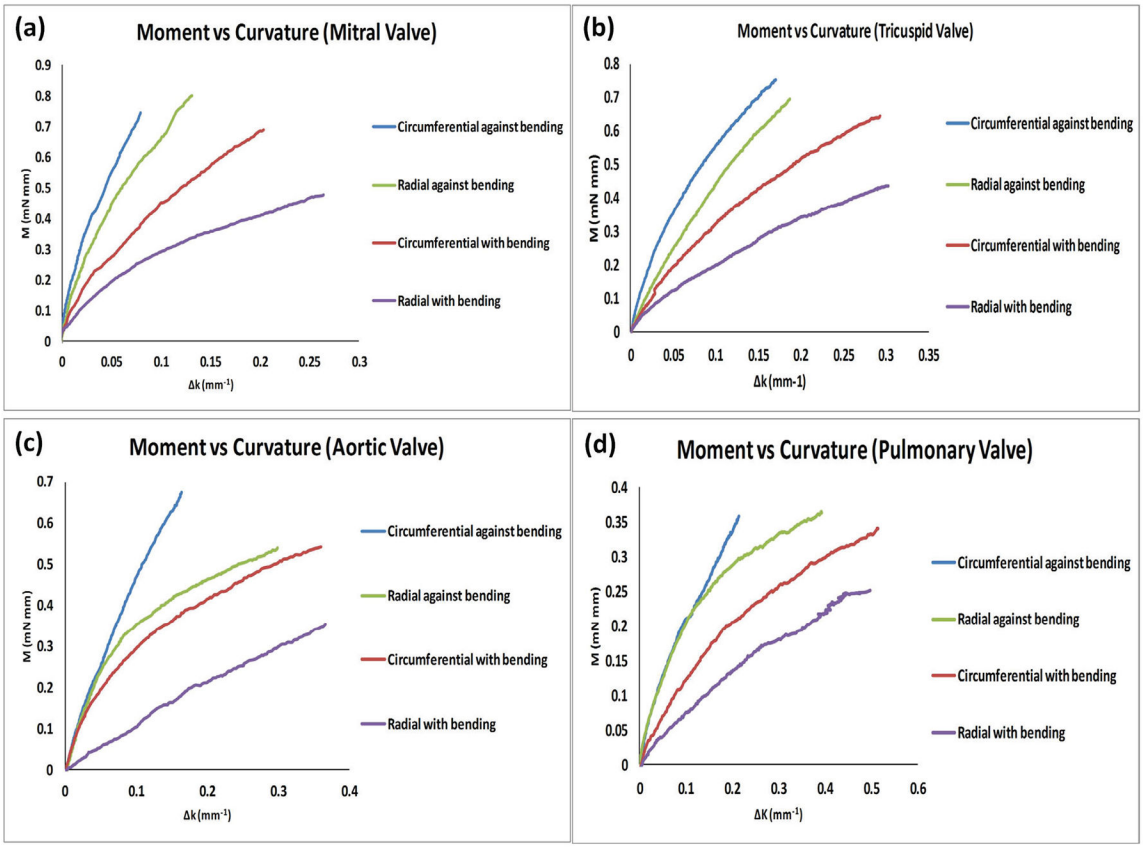

FIG. 6:

With-curvature bending and against-curvature bending were plotted in one coordinate quadrant for comparing AC circumferential, AC radial, WC circumferential, and WC radial bending in (a) mitral valve leaflets, (b) tricuspid valve leaflets, (c) aortic valve leaflets, and (d) pulmonary valve leaflets.

TABLE 1:

EI values (flexural rigidity) at curvature of 0.025 mm^{-1}, 0.05 mm^{-1}, and 0.075 mm^{-1} for the four types of valve leaflets. Data was shown as average ± standard error.

Curvature (mm)	Mitral Valve Leaflet EI ($mN*mm^2$)				Tricuspid Valve Leaflet EI ($mN*mm^2$)				Aortic Valve Leaflet EI ($mN*mm^2$)				Pulmonary Valve Leaflet EI ($mN*mm^2$)			
	Circumferential		Radial		Circumferential		Radial		Circumferential		Radial		Circumferential		Radial	
	AC	wc	AC	WC	AC	WC	AC	WC	AC	WC	AC	WC	AC	WC	AC	WC
0.025	15.611 ± 3.385	6.994 ± 1.447	15.263 ± 6.841	5.60 ± 1.701	11.184 ± 3.459	5.907 ± 2.179	8.135 ± 2.751	3.442 ± 1.209	5.835 ± 0.449	4.379 ± 1.33	6.293 ± 2.255	1.217 ± 0.401	3.05 ± 0.535	2.234 ± 1.093	2.986 ± 0.425	1.093 ± 0.354
0.05	12.960 ± 2.977	5.843 ± 1.228	10.843 ± 3.623	4.852 ± 1.55	9.819 ± 3.302	6.374 ± 2.808	7.27 ± 2.307	2.713 ± 0.675	5.277 ± 0.681	3.446 ± 0.956	5.286 ± 1.867	1.189 ± 0.185	2.737 ± 0.476	1.772 ± 0.829	2.515 ± 0.316	0.841 ± 0.262
0.075	5.752 ± 0.307	5.199 ± 1.126	6.695 ± 0.967	3.219 ± 0.993	6.219 ± 1.524	3.568 ± 1.435	6.934 ± 2.236	2.393 ± 0.561	5.162 ± 0.554	2.911 ± 0.833	3.148 ± 0.382	1.303 ± 0.211	2.283 ± 0.367	1.333± 0.754	2.23 ± 0.207	0.763 ± 0.219

TABLE 2:

EI values (instantaneous effective bending modulus) at curvature of 0.025 mm^{-1}, 0.05 mm^{-1}, and 0.075 mm^{-1} for the four types of valve leaflets. Data was shown as average ± standard error.

Curvature (mm)	Mitral Valve Leaflet E (kPa, or $mN*mm^{-2}$)				Tricuspid Valve Leaflet E (kPa, or $mN*mm^{-2}$)				Aortic Valve Leaflet E (kPa, or $mN*mm^{-2}$)				Pulmonary Valve Leaflet E (kPa, or $mN*mm^{-2}$)			
	Circumferential		Radial		Circumferential		Radial		Circumferential		Radial		Circumferential		Radial	
	AC	WC	AC	WC	AC	WC	AC	WC	AC	WC	AC	WC	AC	WC	AC	WC
0.025	65.394 ± 14.723	28.745 ± 5.763	71.360 ± 19.391	30.767 ± 8.117	88.754 ± 20.824	49.918 ± 16.83	81.484 ± 24.478	36.184 ± 10.862	231.548 ± 28.467	159.169 ± 36.606	421.776 ± 72.193	97.227 ± 35.124	778.672 ± 127.156	498.163 ± 196.993	1808.30 ± 209.673	698.290 ± 112.717
0.05	53.942 ± 12.802	23.844 ± 4.526	59.422 ± 16.161	25.96 ± 6.573	77.865 ± 19.938	52.712 ± 18.797	73.003 ± 20.677	28.842 ± 5.462	211.730 ± 39.987	125.926 ± 26.152	353.038 ± 58.820	95.338 ± 21.538	697.119 ± 114.716	403.410 ± 144.165	1531.84 ± 163.170	523.604 ± 70.149
0.075	22.944 ± 2.290	21.185 ± 4.117	39.804 ± 5.336	18.668 ± 0.993	55.764 ± 13.938	34.33 ± 13.938	69.591 ± 20.182	25.402 ± 4.396	207.233 ± 36.111	106.962 ± 23.601	260.268 ± 17.420	105.434 ± 25.118	624.291 ± 140.784	361.498 ± 124.637	1419.33 ± 104.265	384.956 ± 103.984

J Long Term Eff Med Implants. Author manuscript; available in PMC 2019 September 04.